PHILOSOPHICAL TRANSACTIONS OF THE ROYAL SOCIETY A MATHEMATICAL, PHYSICAL & ENGINEERING SCIENCES

Solution of the Boltzmann Equation for a Reacting Gas Mixture

Georg Kugerl

Phil. Trans. R. Soc. Lond. A 1993 **342**, 413-438
doi: 10.1098/rsta.1993.0027

Solution of the Boltzmann equation for a reacting gas mixture†

By Georg Kügerl

Institute for Theoretical Physics, Graz University of Technology, Petersgasse 16, A-8010 Graz, Austria

Contents

A spatially homogeneous gas mixture consisting of structureless molecules of kind A, B, C, D is considered in which the reversible bimolecular reaction A+B $\rightleftharpoons$ C+D occurs. The Boltzmann equation describing this model gas is solved numerically by using the multigroup method. The collision cross sections correspond to the reactive hard sphere model. Parameters are the heat of reaction, the activation energy and the steric factor. Emphasis in the presentation of the results is laid on highly exothermic reactions with large activation energy, in which case the gas undergoes a thermal explosion. It is found that the corrections of the chemical

† This paper was produced from the author's disk by using the TEX typesetting system.

Phil. Trans. R. Soc. Lond. A (1993) **342**, 413–438
Printed in Great Britain

rate constants due to translational non-equilibrium effects are noticeable. The result is a shortening of the reaction period by up to 25%.

1. Introduction

In the collision theory approach to the calculation of chemical reaction rates it is usually assumed that the distribution functions of translational and internal degrees of freedom are in thermal equilibrium. A chemical reaction, however, perturbs the Maxwell–Boltzmann distributions and affects therefore in turn the rate of reaction. In the case of translational degrees of freedom, the determination of this non-equilibrium effect requires the solution of the Boltzmann equation.

The influence of perturbed velocity distribution functions on the rate of chemical reactions has been investigated on the basis of the Boltzmann equation in a number of treatments (see, for example, Shizgal & Karplus 1970; Shizgal 1971; Boffi & Rossani 1990; and references herein). In most of these studies the effect of the activation energy on the velocity distribution of the reacting particles was considered. An energy threshhold for reactive collisions results in a depletion of hot molecules, and thus reduces the reaction rate in comparison to the equilibrium rate. Quantitative assessments of this non-equilibrium effect conclude that the resulting corrections are small. The molecular-kinetic situation is completely different if in addition to the activation energy a large heat of reaction is taken into consideration. Then the thermalization of 'hot' product molecules in the 'cold' reactant gas leads to an overpopulation of the reactant particle distribution function at high molecular energies. This effect may overcome the aforementioned depletion of hot molecules. The result is an increase in the rate of chemical reaction. The effect of the heat of reaction on the velocity distribution functions has been studied quantitatively by Prigogine & Mahieu (1950) using the Chapman–Enskog procedure for solving the Boltzmann equation. It was pointed out that the heat of reaction increases the reaction rate to an appreciable extent. Koura (1973) has used a Monte Carlo method to describe a highly exothermic reaction with low activation energy. He found that the reaction rate can be increased by more than 100%.

From a practical point of view, an important case seems to be a chemical reaction with high activation energy and large heat release, as is the case in combustion type reactions. For this situation, no solutions of the Boltzmann equation have been obtained so far, and the extent of the non-equilibrium effects on the chemical rate constants is unknown. The aforementioned methods for solving the Boltzmann equation fail if a large heat of reaction and a high activation energy are taken into account: the applicability of the usual Sonine polynomial subapproximation used in the Chapman–Enskog procedure is restricted to small perturbations of the velocity distributions. The more flexible Monte Carlo technique faces the problem that in the case of high activation energies only a tiny fraction of collisions are reactive. Hence a large number of sample particles are required for an accurate modelling of the reaction process making heavy demands on the computational facilities. Recently, a consistent numerical method for the solution of the nonlinear Boltzmann equation applicable to gases with chemical reactions has been introduced (Kügerl 1991). This multigroup method reduces

PHILOSOPHICAL TRANSACTIONS OF THE ROYAL SOCIETY A MATHEMATICAL, PHYSICAL & ENGINEERING SCIENCES

the solution of the Boltzmann equation to the numerical solution of a system of ordinary differential equations. The method also allows long time integration of the Boltzmann equation by using stiff ODE solvers.

In the present paper a spatially homogeneous gas consisting of the chemical species A, B, C and D is considered, in which a reversible bimolecular reaction of the from

$$\mathrm{A} + \mathrm{B} \rightleftharpoons \mathrm{C} + \mathrm{D} \tag{1.1}$$

occurs. In this reaction, a large amount of heat is released in the forward direction. It is assumed that the molecules of each species are structureless and that they all have the same mass. The multigroup method is used to solve the Boltzmann equation of this model gas for various values of the heat of reaction and the activation energy.

To this *microscopic* formulation of gas-phase reactions corresponds a *macroscopic* approach involving the concepts of rate coefficients and a thermodynamic temperature. In this work the reaction cross sections are chosen such that the rate coefficients for the reaction (1.1) obey the well-known Arrhenius law. It is the purpose of the present research to demonstrate the discrepancies in the two different levels of description by comparing the density profiles obtained from the Boltzmann equation with the solutions of the chemical rate equations.

2. Basic equations

(*a*) *The Boltzmann equation*

The one-particle velocity distribution functions $f_\alpha(\boldsymbol{v}_1, t)$, $\alpha = \mathrm{A}, \mathrm{B}, \mathrm{C}, \mathrm{D}$, are assumed to be governed by the Boltzmann equation (cf. Ross & Mazur 1961; Light *et al.* 1969)

$$\frac{\partial}{\partial t}\begin{bmatrix} f_{\mathrm{A}} \\ f_{\mathrm{B}} \\ f_{\mathrm{C}} \\ f_{\mathrm{D}} \end{bmatrix} = \sum_{\beta=\mathrm{A},\ldots,\mathrm{D}} \begin{bmatrix} J_{\mathrm{A}\beta}^{\mathrm{A}\beta} \\ J_{\mathrm{B}\beta}^{\mathrm{B}\beta} \\ J_{\mathrm{C}\beta}^{\mathrm{C}\beta} \\ J_{\mathrm{D}\beta}^{\mathrm{D}\beta} \end{bmatrix} + \begin{bmatrix} J_{\mathrm{CD}}^{\mathrm{AB}} \\ J_{\mathrm{DC}}^{\mathrm{BA}} \\ J_{\mathrm{AB}}^{\mathrm{CD}} \\ J_{\mathrm{BA}}^{\mathrm{DC}} \end{bmatrix} \tag{2.1}$$

with

$$J_{\gamma\delta}^{\alpha\beta} = \int \mathrm{d}\boldsymbol{v}_2 \int \mathrm{d}\Omega \; g_{\alpha\beta} I_{\alpha\beta}^{\gamma\delta}(g_{\alpha\beta}, \Omega) \left[f_\gamma(\boldsymbol{v}_1', t) f_\delta(\boldsymbol{v}_2', t) - f_\alpha(\boldsymbol{v}_1, t) f_\beta(\boldsymbol{v}_2, t) \right] . \tag{2.2}$$

Here, $I_{\alpha\beta}^{\gamma\delta}$ is the differential cross section for the transition $(\alpha, \beta) \to (\gamma, \delta)$, $g_{\alpha\beta}$ is the relative velocity of the colliding particles α and β, and Ω is the solid scattering angle. The first term on the right-hand side of equation (2.1) describes the rate of change of the distribution functions due to elastic collisions. The second term is the collision integral for reactive collisions.

The normalization of f_α is chosen such that the particle density and the density

of kinetic energy are defined by

$$\begin{pmatrix} n_\alpha \\ \frac{3}{2} n_\alpha \kappa T_\alpha \end{pmatrix} = \int \mathrm{d}\boldsymbol{v} \begin{pmatrix} 1 \\ \frac{1}{2} m v^2 \end{pmatrix} f_\alpha(\boldsymbol{v}, t), \tag{2.3}$$

where κ is the Boltzmann constant, m is the particle mass and T_α denotes the temperature of component α. According to the Boltzmann equation there exists the following relationship among the reaction rates,

$$\frac{\mathrm{d}n_\mathrm{A}}{\mathrm{d}t} = \frac{\mathrm{d}n_\mathrm{B}}{\mathrm{d}t} = -\frac{\mathrm{d}n_\mathrm{C}}{\mathrm{d}t} = -\frac{\mathrm{d}n_\mathrm{D}}{\mathrm{d}t}, \tag{2.4}$$

which corresponds with the reaction mechanism (1.1). For the rates of change of the overall values

$$\begin{pmatrix} n \\ \frac{3}{2} n \kappa T \end{pmatrix} = \sum_{\alpha=\mathrm{A},\ldots,\mathrm{D}} \begin{pmatrix} n_\alpha \\ \frac{3}{2} n_\alpha \kappa T_\alpha \end{pmatrix} \tag{2.5}$$

one finds

$$\mathrm{d}n/\mathrm{d}t = 0 \tag{2.6}$$

and

$$\tfrac{3}{2} n \kappa \frac{\mathrm{d}T}{\mathrm{d}t} = Q \frac{\mathrm{d}n_\mathrm{C}}{\mathrm{d}t}, \tag{2.7}$$

where Q is the molecular heat of reaction. Equation (2.7) reflects the fact that the reaction process under consideration is adiabatic; each molecular reaction in forward (reverse) direction increases (decreases) the internal energy of the gas by the amount of heat Q.

The solution of the Boltzmann equation (2.1) obeys an H-theorem (see, for example, Polak & Khachoyan 1985), according to which the equilibrium solution must be of the form

$$f_\alpha^{\mathrm{eq}}(\boldsymbol{v}) = n_\alpha^{\mathrm{eq}} \left(\frac{m}{2\pi\kappa T} \right)^{3/2} \exp\left(-\frac{m v^2}{2\kappa T} \right), \quad \alpha = \mathrm{A}, \mathrm{B}, \mathrm{C}, \mathrm{D}, \tag{2.8}$$

where the equilibrium densities satisfy the law of mass action

$$\frac{n_\mathrm{C}^{\mathrm{eq}} n_\mathrm{D}^{\mathrm{eq}}}{n_\mathrm{A}^{\mathrm{eq}} n_\mathrm{B}^{\mathrm{eq}}} = \exp\left(\frac{Q}{\kappa T} \right). \tag{2.9}$$

The steady state (2.8) with (2.9) defines chemical equilibrium. It is convenient to speak of a further kind of equilibrium, where the distribution functions also take the form of a maxwellian but where the densities and the temperature have not yet reached their final values. We shall refer to this situation as 'kinetic equilibrium'.

(*b*) *Cross sections*

(i) *Total cross section*

If two molecules α and β collide, the result may be an elastic scattering or a chemical reaction. The total cross section $\sigma_{\alpha\beta}$ consists therefore of an elastic and a reactive part,

$$\sigma_{\alpha\beta}(E) = \sigma_{\mathrm{el}}(E) + \sigma_{\mathrm{r}}(E). \tag{2.10}$$

For the following, an isotropic scattering angle distribution is assumed. The relation between the integral and the differential cross section for the transition $(\alpha, \beta) \rightarrow (\gamma, \delta)$ then reads

$$\sigma_{\alpha\beta}^{\gamma\delta}(E) = 4\pi I_{\alpha\beta}^{\gamma\delta}(g_{\alpha\beta}), \tag{2.11}$$

with E being the relative energy of the colliding particles, $E = \frac{1}{4} m {g_{\alpha\beta}}^2$.

In choosing the energy dependence of the cross sections we start with the total cross section which we assume to be constant:

$$\sigma_{\alpha\beta}(E) = \sigma. \tag{2.12}$$

This hard sphere model has the advantage of yielding a simple expression for the dimensionless equilibrium reaction rate constants (see below). This is essential for the comparison of the density plots obtained from the Boltzmann equation with those obtained from the chemical rate equations, which is the main goal of the present work.

(ii) *Reaction cross sections*

For the reaction cross sections in forward and in reverse direction,

$$\sigma_{\mathrm{f}} \equiv \sigma_{\mathrm{AB}}^{\mathrm{CD}}, \qquad \sigma_{\mathrm{r}} \equiv \sigma_{\mathrm{CD}}^{\mathrm{AB}}, \tag{2.13}$$

respectively, we choose the reactive hard sphere model (cf. Light *et al.* 1969)

$$\sigma_{\mathrm{f,r}}(E) = \begin{cases} 0 & \text{if} \quad E < E_{\mathrm{f,r}}^*, \\ \hat{\sigma}(1 - E_{\mathrm{f,r}}^*/E) & \text{if} \quad E \geq E_{\mathrm{f,r}}^*. \end{cases} \tag{2.14}$$

In this model reactive scattering in the forward (reverse) direction is said to occur only if the impact parameter and the initial kinetic energy of the colliding particles are such that on impact the energy along the line of centres exceeds a threshold value E_{f}^* (E_{r}^*). The molecular activation energies E_{f}^* and E_{r}^* are related to the heat of reaction by

$$E_{\mathrm{r}}^* - E_{\mathrm{f}}^* = Q. \tag{2.15}$$

The reactive hard sphere model satisfies the principle of microscopic reversibility (see, for example, Pyun & Ross 1964)

$$E' \sigma_{\mathrm{f}}(E') = E \sigma_{\mathrm{r}}(E), \tag{2.16}$$

with $E = E' + Q$. Here, E' and E are the precollisional and postcollisional relative energies, respectively.

In general not every collision between A and B particles or C and D particles leads to a reaction, even if the kinetic energy is sufficient. A reaction cannot occur, for instance, if the geometrical orientation of the colliding particles is not favourable for product formation. The maximum reaction probability

$$P = \hat{\sigma}/\sigma \tag{2.17}$$

is called the steric factor (cf. Kondrat'ev 1964).

(iii) *Cross sections for elastic scattering*

Having now chosen the total and the reaction cross sections, the cross sections for elastic scattering follow from equation (2.10). For all those collisions

which cannot result in a chemical reaction, the elastic scattering cross section is constant:

$$\sigma_{\alpha\alpha}^{\alpha\alpha} = \sigma_{\mathrm{AC}}^{\mathrm{AC}} = \sigma_{\mathrm{AD}}^{\mathrm{AD}} = \sigma_{\mathrm{BC}}^{\mathrm{BC}} = \sigma_{\mathrm{BD}}^{\mathrm{BD}} = \sigma, \qquad \alpha = \mathrm{A}, \ldots, \mathrm{D}. \tag{2.18}$$

However, if the outcome of a collision can be either an elastic scattering or a reaction, one has

$$\sigma_{\mathrm{AB}}^{\mathrm{AB}}(E) = \sigma - \sigma_{\mathrm{f}}(E), \tag{2.19}$$

$$\sigma_{\mathrm{CD}}^{\mathrm{CD}}(E) = \sigma - \sigma_{\mathrm{r}}(E). \tag{2.20}$$

Note that the cross sections for elastic scattering of the type (A,B) → (A,B) or (C,D) → (C,D) are not constant, but rather decrease above the respective activation energy asymptotically to the constant value $(1 - P)\sigma$.

(c) *Chemical rate equations*

Finally in this section, the continuum-based description of this model gas is presented. The density of each species is governed by a rate equation, which for component C, for instance, reads

$$\mathrm{d}n_{\mathrm{C}}/\mathrm{d}t = k_{\mathrm{f}} n_{\mathrm{A}} n_{\mathrm{B}} - k_{\mathrm{r}} n_{\mathrm{C}} n_{\mathrm{D}}. \tag{2.21}$$

The reaction rate constants k_{f} and k_{r} are usually assumed to depend on temperature only, i.e. they do not depend explicitly on the density or on time, $k \neq k(n_\alpha, t)$.

Because of equation (2.4) the single equation (2.21) is sufficient to describe the present reaction process. An expression for the temperature in terms of the product density n_{C} can be found by considering the adiabatic nature of the reaction process. Integration of equation (2.7) yields

$$\tfrac{3}{2} n \kappa T(t) = \tfrac{3}{2} n \kappa T_0 + Q\left[n_{\mathrm{C}}(t) - n_{\mathrm{C}0}\right], \tag{2.22}$$

where $(n_{\mathrm{C}0}, T_0)$ are the initial values of (n_{C}, T).

It is well known that the relationship among the chemical rate equations and the Boltzmann equation can be made by defining the rate constant in the forward direction by

$$k_{\mathrm{f}} = \frac{1}{n_{\mathrm{A}} n_{\mathrm{B}}} \int \mathrm{d}\boldsymbol{v}_1 \int \mathrm{d}\boldsymbol{v}_2 \, g \sigma_{\mathrm{f}}(\tfrac{1}{4} m g^2) f_{\mathrm{A}}(\boldsymbol{v}_1, t) f_{\mathrm{B}}(\boldsymbol{v}_2, t), \tag{2.23}$$

with $g = |\boldsymbol{v}_1 - \boldsymbol{v}_2|$. The reverse reaction rate k_{r} is given by a similar expression. It can readily be seen from equation (2.23) that the rate constant depends on the velocity distribution function of the reactants. The assumption $k = k(T)$ is therefore in general not valid. However, if the gas is in kinetic equilibrium the rate constants are functions of the temperature alone. Using the reactive hard sphere model one obtains (see, for example, Light *et al.* 1969)

$$k_{\mathrm{f,r}}^{(0)} = \frac{P\nu(T)}{n} \exp\left(-\frac{E_{\mathrm{f,r}}^*}{\kappa T}\right). \tag{2.24}$$

Hence, the equilibrium rate constants $k_{\mathrm{f,r}}^{(0)}$ for reactive hard spheres have the well-known form of the Arrhenius law, with a pre-exponential factor proportional to the collision frequency

$$\nu(T) = n\sigma(16\kappa T/\pi m)^{1/2}. \tag{2.25}$$

In a dimensionless representation where time is measured in units of the mean collision time at the reference temperature T_0 and density is given in units of the total density, the rate constants read

$$k_{\mathrm{f,r}}^{(0)'}(T) = P\,(T/T_0)^{1/2} \exp\left(-E_{\mathrm{f,r}}^{*}/\kappa T\right). \tag{2.26}$$

The dimensionless forward rate constant $k_{\mathrm{f}}^{(0)'}(T_0)$ is the probability that a collision between an A and a B particle results in a reaction, provided that the reactant particle velocity distribution is a maxwellian with temperature T_0. In the case of a small steric factor or a high activation energy this probability is small, and the chemical reaction is slow in terms of the collision frequency. In § 4 we investigate whether a small value of $k_{\mathrm{f}}^{(0)'}$ necessarily justifies the equilibrium assumption usually made for the translational mode.

3. Numerical method of solution

(*a*) *Scalar form of the Boltzmann equation*

For the idealized geometrical situation considered in this work, the structure of the Boltzmann collision operator (2.2) can be simplified substantially. By assuming the velocity distribution functions to be isotropic, $f_\alpha(\boldsymbol{v}, t) = f_\alpha(v, t), \alpha = \mathrm{A}, \mathrm{B}, \mathrm{C}, \mathrm{D}$, the fivefold integral in equation (2.2) can be reduced to a twofold integral. The remaining equation is the so-called 'scalar Boltzmann equation' (cf. Ziff (1980), Ernst (1981) and Kügerl (1989) for the non-reactive case). It will be the starting point for the numerical solution of the Boltzmann equation.

It is convenient to change from the velocity representation to the energy representation of the distribution function by the transformation

$$(m^3 x)^{1/2} G_\alpha(x, t)\,\mathrm{d}x = 4\pi v^2 f_\alpha(v, t)\,\mathrm{d}v, \tag{3.1}$$

with $x = \frac{1}{2}mv^2$. The equilibrium distribution function then reads for instance

$$G_\alpha^{\mathrm{eq}}(x; n_\alpha, T) = \frac{2n_\alpha}{\sqrt{\pi}}(m\kappa T)^{-3/2} \exp\left(-\frac{x}{\kappa T}\right). \tag{3.2}$$

According to the transformation (3.1), the Boltzmann equation (2.1) can be written in the form (cf. Kügerl 1991)

$$(m^3 x_1)^{1/2} \frac{\partial}{\partial t} \begin{bmatrix} G_{\mathrm{A}} \\ G_{\mathrm{B}} \\ G_{\mathrm{C}} \\ G_{\mathrm{D}} \end{bmatrix} = \sum_{\beta=\mathrm{A},\ldots,\mathrm{D}} \begin{bmatrix} J_{\mathrm{A}\beta}^{\mathrm{A}\beta} \\ J_{\mathrm{B}\beta}^{\mathrm{B}\beta} \\ J_{\mathrm{C}\beta}^{\mathrm{C}\beta} \\ J_{\mathrm{D}\beta}^{\mathrm{D}\beta} \end{bmatrix} + \begin{bmatrix} J_{\mathrm{CD}}^{\mathrm{AB}} \\ J_{\mathrm{DC}}^{\mathrm{BA}} \\ J_{\mathrm{AB}}^{\mathrm{CD}} \\ J_{\mathrm{BA}}^{\mathrm{DC}} \end{bmatrix} \tag{3.3}$$

with the collision integral

$$J^{\alpha\beta}_{\gamma\delta} = \int_0^\infty \mathrm{d}x_1' \int_0^\infty \mathrm{d}x_2'\; R^{\alpha\beta}_{\gamma\delta}(x_1', x_2'|x_1) \times \left[G_\gamma(x_1', t)G_\delta(x_2', t) - G_\alpha(x_1, t)G_\beta(x_1' + x_2' - x_1 + Q^{\alpha\beta}_{\gamma\delta}, t)\right]. \quad (3.4)$$

The scalar scattering kernel is defined by

$$R^{\alpha\beta}_{\gamma\delta}(x_1', x_2'|x_1) = \frac{m^7}{32\pi^3} \int \mathrm{d}\boldsymbol{v}_1 \int \mathrm{d}\boldsymbol{v}_2 \int \mathrm{d}\boldsymbol{v}_1' \int \mathrm{d}\boldsymbol{v}_2' \frac{g'}{g} \sigma^{\alpha\beta}_{\gamma\delta}(\tfrac{1}{4}mg'^2) \times \delta(\boldsymbol{v}_1' + \boldsymbol{v}_2' - \boldsymbol{v}_1 - \boldsymbol{v}_2)\delta\left(\tfrac{1}{4}mg'^2 - \tfrac{1}{4}mg^2 + Q^{\alpha\beta}_{\gamma\delta}\right) \times \delta\left(x_1 - \tfrac{1}{2}mv_1^2\right)\delta\left(x_1' - \tfrac{1}{2}mv_1'^2\right)\delta\left(x_2' - \tfrac{1}{2}mv_2'^2\right), \quad (3.5)$$

with $g' = |\boldsymbol{v}_1' - \boldsymbol{v}_2'|$ and $g = |\boldsymbol{v}_1 - \boldsymbol{v}_2|$. The quantity $Q^{\alpha\beta}_{\gamma\delta}$ denotes the heat of reaction which is released in the bimolecular transition $(\gamma, \delta) \to (\alpha, \beta)$. One has

$$Q^{\alpha\beta}_{\gamma\delta} = 0 \quad \text{for elastic scattering}, \qquad Q^{\mathrm{CD}}_{\mathrm{AB}} = Q, \qquad Q^{\mathrm{AB}}_{\mathrm{CD}} = -Q, \quad (3.6)$$

with $Q^{\alpha\beta}_{\gamma\delta} = Q^{\beta\alpha}_{\delta\gamma}$.

The scalar scattering kernel $R^{\alpha\beta}_{\gamma\delta}(x_1', x_2'|x_1)$ describes the probability density for the transition of two particles (γ, δ) with energies (x_1', x_2') to particles of kind (α, β) with energies $(x_1, x_1' + x_2' - x_1 + Q^{\alpha\beta}_{\gamma\delta})$. For isotropic cross sections, as considered in this paper, the multiple integral (3.5) can always be reduced to a onefold integral. For the cross sections introduced in § 2 *b*, even the remaining integral can be evaluated analytically, so that a closed representation of all scalar scattering kernels is possible. The results are presented in Appendix A.

(*b*) *Multigroup method*

For the numerical solution of equation (3.3) the 'multigroup method' is used. This numerical procedure proved to be very efficient for solving the (linear) neutron transport equation (see, for instance, Bell & Glasstone 1970). Recently, its range of application has been extended to nonlinear transport problems (Kügerl & Schürrer 1990).

The molecular energy axis $0 \leq x < \infty$ is restricted to a finite interval $[0, x_N]$ which is then discretized into a uniform grid with the grid points

$$\bar{x}_i = \Delta x\,(i - \tfrac{1}{2}), \quad i = 1, 2, \ldots, N, \quad (3.7)$$

with $\Delta x = x_N/N$. According to this discretization, the distribution function is replaced by the grid function

$$G^i_\alpha(t) = G_\alpha(\bar{x}_i, t), \quad i = 1, 2, \ldots, N, \quad (3.8)$$

and the scalar scattering kernel is reduced to the scattering coefficients

$$\left(R^{\alpha\beta}_{\gamma\delta}\right)^i_{kl} = R^{\alpha\beta}_{\gamma\delta}(\bar{x}_k, \bar{x}_l|\bar{x}_i), \quad i, k, l = 1, 2, \ldots, N. \quad (3.9)$$

The restriction to a uniform grid further requires that the heat of reaction and the activation energies are integer multiples of Δx. In the case of the heat of

reaction this assumption reads

$$Q = q\,\Delta x, \qquad q = 0, 1, 2, 3, \ldots \tag{3.10}$$

All integrals over the molecular energy variable x are now approximated by the composite midpoint rule,

$$\int_0^\infty \mathrm{d}x\,\varphi(x) \approx \Delta x \sum_{i=1}^{N} \varphi(\bar{x}_i). \tag{3.11}$$

Through this approximation, the particle and kinetic energy densities are defined by (cf. equations (2.3), (3.1) and (3.8))

$$\begin{pmatrix} n_\alpha \\ \frac{3}{2} n_\alpha \kappa T_\alpha \end{pmatrix} = \Delta x\, m^{3/2} \sum_{i=1}^{N} \bar{x}_i^{1/2} \begin{pmatrix} 1 \\ \bar{x}_i \end{pmatrix} G_\alpha^i(t). \tag{3.12}$$

By applying the composite midpoint rule to the Boltzmann equation, one obtains the following system of ODEs

$$(m^3\bar{x}_i)^{1/2} \frac{\mathrm{d}}{\mathrm{d}t} \begin{bmatrix} G_\mathrm{A}^i \\ G_\mathrm{B}^i \\ G_\mathrm{C}^i \\ G_\mathrm{D}^i \end{bmatrix} = \sum_{\beta=\mathrm{A},\ldots,\mathrm{D}} \begin{bmatrix} (J_{\mathrm{A}\beta}^{\mathrm{A}\beta})_i \\ (J_{\mathrm{B}\beta}^{\mathrm{B}\beta})_i \\ (J_{\mathrm{C}\beta}^{\mathrm{C}\beta})_i \\ (J_{\mathrm{D}\beta}^{\mathrm{D}\beta})_i \end{bmatrix} + \begin{bmatrix} (J_{\mathrm{CD}}^{\mathrm{AB}})_i \\ (J_{\mathrm{DC}}^{\mathrm{BA}})_i \\ (J_{\mathrm{AB}}^{\mathrm{CD}})_i \\ (J_{\mathrm{BA}}^{\mathrm{DC}})_i \end{bmatrix}, \tag{3.13}$$

where $i = 1, 2, \ldots, N$. The collision 'integrals' are defined by

$$(J_{\gamma\delta}^{\alpha\beta})_i = \Delta x^2 \sum_{k,l=1}^{N} \left(R_{\gamma\delta}^{\alpha\beta}\right)_{kl}^{i} (G_\gamma^k G_\delta^l - G_\alpha^i G_\beta^{k+l-i+q'}), \tag{3.14}$$

with

$$q' = Q_{\gamma\delta}^{\alpha\beta}/\Delta x. \tag{3.15}$$

This multigroup method has the favourable property that all the fundamental characteristics of the Boltzmann equation are preserved (cf. Kügerl 1991). The solutions of equation (3.13) conserve particle number and energy, and they obey an H-theorem. Moreover, it can be shown that the equilibrium solution must have the form

$$\Gamma_\alpha^i(n_\alpha^{\mathrm{eq}}, T) = \frac{n_\alpha^{\mathrm{eq}}}{m^{3/2} S(B)} \exp(-B\bar{x}_i), \tag{3.16}$$

where the equilibrium densities satisfy the law of mass action

$$\frac{n_\mathrm{C}^{\mathrm{eq}} n_\mathrm{D}^{\mathrm{eq}}}{n_\mathrm{A}^{\mathrm{eq}} n_\mathrm{B}^{\mathrm{eq}}} = \exp(Bq\,\Delta x). \tag{3.17}$$

The quantity B is defined in terms of the temperature through the nonlinear

equation

$$\sum_{i=1}^{N} \bar{x}_i^{1/2} \left(\bar{x}_i - \tfrac{3}{2}\kappa T\right) \exp(-B\bar{x}_i) = 0, \tag{3.18}$$

and $S(B)$ is given by

$$S(B) = \Delta x \sum_{i=1}^{N} \bar{x}_i^{1/2} \exp(-B\bar{x}_i). \tag{3.19}$$

As demonstrated in Kügerl (1991) by means of a numerical example, B and $S(B)$ converge rapidly to $1/\kappa T$ and $\frac{1}{2}\pi^{1/2}B^{-3/2}$, respectively, for decreasing Δx and sufficiently large x_N, a result of the second-order accuracy of the composite midpoint rule. Hence the equilibrium solution (3.16) can be called a discretized maxwellian (cf. equations (3.2) and (3.16)).

(c) *Initial conditions*

The initial state of the gas is chosen to be a pure stoichiometric mixture of the reactants,

$$n_{\mathrm{A}0} = n_{\mathrm{B}0} = \tfrac{1}{2}n, \tag{3.20}$$

$$n_{\mathrm{C}0} = n_{\mathrm{D}0} = 0, \tag{3.21}$$

with both components A and B having the same initial temperature T_0. As a result of equations (3.20) and (3.21) one has $n_{\mathrm{C}} = n_{\mathrm{D}} = \frac{1}{2}n - n_{\mathrm{A}} = \frac{1}{2}n - n_{\mathrm{B}}$ for all times. The initial velocity distribution functions are taken to be maxwellians (2.8) with number density $n_{\alpha 0}$ and temperature T_0. The initial values of the grid functions (see equation (3.8)) for the multigroup equations (3.13) then read (cf. equation (3.16))

$$G^i_{\mathrm{A}0} = G^i_{\mathrm{B}0} = \frac{n}{2m^{3/2}S_0} \exp(-B_0\bar{x}_i), \quad i = 1, 2, \ldots, N, \tag{3.22}$$

$$G^i_{\mathrm{C}0} = G^i_{\mathrm{D}0} = 0, \quad i = 1, 2, \ldots, N; \tag{3.23}$$

B_0 is found as the zero of equation (3.18) with $T = T_0$; S_0 then follows from equation (3.19).

Using the various cross sections introduced in § 2 *b*, it can be deduced from the Boltzmann equation (2.1) that if $f_{\mathrm{A}} = f_{\mathrm{B}}$, $f_{\mathrm{C}} = f_{\mathrm{D}}$ at some initial time, this symmetry holds for all future times. The special choice of initial conditions implies therefore that

$$G^i_{\mathrm{A}}(t) = G^i_{\mathrm{B}}(t), \quad G^i_{\mathrm{C}}(t) = G^i_{\mathrm{D}}(t) \tag{3.24}$$

for all times $t \geq 0$. Note that this conclusion also depends on the fact that all particles are assumed to have equal mass. As a result of the symmetry (3.24), the dimension of the set of multigroup equations (3.13) can be reduced from $4N$ to $2N$.

(d) *On the choice of the cut-off energy* x_N

Before moving to the numerical solution of equation (3.13), a few 'technical details' arising in the multigroup method must be clarified. The first concerns

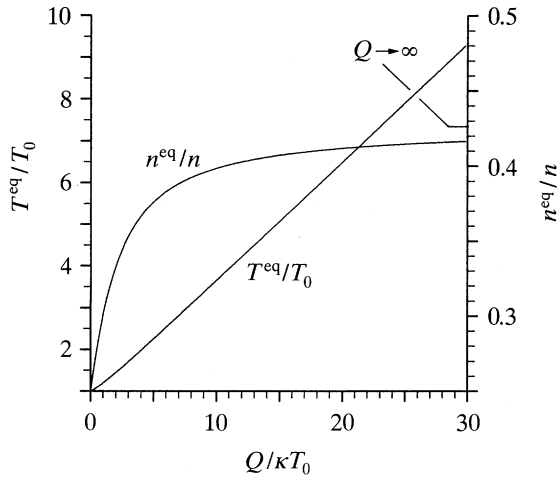

Figure 1. Equilibrium product density and temperature against heat of reaction.

the choice of the cut-off energy x_N. It is clear that x_N must be large enough so that particles 'hotter' than x_N can be ignored in regard to their contribution to the gas-dynamical effects. In practice this means that one has to increase x_N until a sufficient convergence of the numerical results is achieved. However, a good estimate for the cut-off energy can be found on physical grounds. To this end consider the temperature increase during the reaction process. The equilibrium value of the reactant density n_C^{eq} is found as the zero of the equation (cf. equations (2.9) and (2.22))

$$\frac{(n_C^{eq}/n)^2}{(\frac{1}{2} - n_C^{eq}/n)^2} = \exp\left(\frac{Q/\kappa T_0}{1 + \frac{2}{3}(Q/\kappa T_0)(n_C^{eq}/n)}\right). \tag{3.25}$$

Substitution of n_C^{eq} into equation (2.22) gives the equilibrium temperature T^{eq}. Figure 1 shows n_C^{eq} and T^{eq} as functions of the heat of reaction.

The value of x_N must be related to the highest temperature reached during the relaxation process, which in the present case is T^{eq}. As far as the density and the temperature at chemical equilibrium are concerned, $x_N = 10\kappa T^{eq}$ is a sufficiently large parameter; cutting-off a maxwellian at $x_N = 10\kappa T$ results in a relative error for n and T of the order of 10^{-4} and 10^{-3}, respectively. An error of this size was accepted in the computations presented in this paper.

Yet it is clear that not necessarily all relevant particles are included within the energy range $0 \leq x \leq 10\kappa T^{eq}$. This is the case if the heat of reaction or the activation energies are greater than $10\kappa T^{eq}$. Since E_r^* is the largest of the values Q, E_f^* and E_r^*, we restrict the following considerations to E_r^*. If $E_r^* > x_N$, then those hot C and D particles which can lead to reverse reactions, are not sufficiently considered by the numerical model. In addition to the above condition we require therefore that $x_N \geq E_r^*$, which leads us to

$$x_N = \max(10\kappa T^{eq}, E_r^*). \tag{3.26}$$

Indeed, equation (3.26) is found to be a good estimate in the sense that the results

Table 1. *Numerical values of collision and reaction rates*

N	$\tilde{\nu}/\nu$	$\tilde{k}_{\mathrm{f}}^{(0)}/k_{\mathrm{f}}^{(0)}$	$\tilde{k}_{\mathrm{r}}^{(0)}/k_{\mathrm{r}}^{(0)}$
20	1.1487	1.0247	1.1198
40	1.0551	1.0241	1.0790
80	1.0187	1.0111	1.0339
160	1.0061	1.0044	1.0130

obtained with a value larger than x_N, say $1.5x_N$, differ only insignificantly from the results obtained with x_N.

(e) *Improvement of the numerical convergence*

In practical applications of the multigroup method, the number of grid points N is restricted to a maximum value depending on the available computer capacity. As a result, the rates on the right-hand side of equation (3.13) are affected with a numerical error which falsifies the speed of the reaction. It is the subject of this subsection to estimate this error and to correct it.

Imagine for the moment, the reaction process is so gentle that the gas is always in perfect kinetic equilibrium. It is clear that then the Boltzmann equation and the chemical rate equations must lead to the same results concerning the densities and the temperature. To find out if that is the case, consider the numerical values for the collision rate (2.25) and the reaction rates (2.24):

$$\tilde{\nu}(T) = \frac{1}{n^2} \sum_{i,k,l=1}^{N} \left(R_{\mathrm{AA}}^{\mathrm{AA}}\right)_{kl}^{i} \Gamma_\alpha^k(n,T)\Gamma_\alpha^l(n,T), \tag{3.27}$$

$$\tilde{k}_{\mathrm{f}}^{(0)}(T) = \frac{1}{n_{\mathrm{A}} n_{\mathrm{B}}} \sum_{i,k,l=1}^{N} \left(R_{\mathrm{AB}}^{\mathrm{CD}}\right)_{kl}^{i} \Gamma_{\mathrm{A}}^k(n_{\mathrm{A}},T)\Gamma_{\mathrm{B}}^l(n_{\mathrm{B}},T), \tag{3.28}$$

$$\tilde{k}_{\mathrm{r}}^{(0)}(T) = \frac{1}{n_{\mathrm{C}} n_{\mathrm{D}}} \sum_{i,k,l=1}^{N} \left(R_{\mathrm{CD}}^{\mathrm{AB}}\right)_{kl}^{i} \Gamma_{\mathrm{C}}^k(n_{\mathrm{C}},T)\Gamma_{\mathrm{D}}^l(n_{\mathrm{D}},T). \tag{3.29}$$

The equilibrium distribution Γ_α^i is given by equation (3.16), and the scattering coefficients are found by inserting equations (A 5), (A 8) or (A 15) into equation (3.9). Table 1 illustrates the relative difference of the numerical values from the exact ones. In this example, $x_N = 20\kappa T$, $Q = E_{\mathrm{f}}^* = 3\kappa T$ was used. A satisfactory convergence for an increasing number of grid points N can be detected. However, table 1 indicates that although the gas is assumed to be in perfect kinetic equilibrium, the numerical solution of the Boltzmann equation and the solution of the chemical rate equation will in general not give the same result. The deviations decrease with increasing N, but a numerical error of a few percent may well be the case in practice.

To eliminate this error, we weight the two terms on the right-hand side of equation (3.13) with the reciprocal of $\tilde{\nu}/\nu$ and $\tilde{k}_{\mathrm{f}}^{(0)}/k_{\mathrm{f}}^{(0)}$, respectively, and obtain

instead

$$(m^3\bar{x}_i)^{1/2}\frac{\mathrm{d}}{\mathrm{d}t}G^i_\alpha = \frac{\nu}{\tilde{\nu}}\sum_{\beta=\mathrm{A},\ldots,\mathrm{D}}(J^{\alpha\beta}_{\alpha\beta})_i + \frac{k^{(0)}_\mathrm{f}}{\tilde{k}^{(0)}_\mathrm{f}}(J^{\alpha\beta}_{\gamma\delta})_i, \tag{3.30}$$

where $\alpha = \mathrm{A}, \mathrm{B}, \mathrm{C}, \mathrm{D}$ and $i = 1, 2, \ldots, N$. Note that $\tilde{\nu}/\nu$ and $\tilde{k}^{(0)}_\mathrm{f}/k^{(0)}_\mathrm{f}$ depend on temperature and therefore implicitly on time.

This correction of the rates has the following effect: if the reaction proceeds too fast, for instance, because of the numerical insufficiency $\tilde{k}^{(0)}_\mathrm{f}/k^{(0)}_\mathrm{f} > 1$, it is slowed down by the factor $k^{(0)}_\mathrm{f}/\tilde{k}^{(0)}_\mathrm{f}$. Similarly, the numerical collision rate $\tilde{\nu}$ is adjusted to the 'true' value ν, by multiplying with $\nu/\tilde{\nu}$. As a result, the numerical error arising from the finite number of grid points, which falsifies the speed of the reaction, is eliminated. We point out that this correction has of course no physical implications, since $\tilde{\nu}/\nu$ and $\tilde{k}^{(0)}_\mathrm{f}/k^{(0)}_\mathrm{f}$ tend to one as N increases. It is introduced only to improve the convergence of the multigroup method.

Two comments are necessary. First, the kinetic equilibrium is disturbed by the reaction. As we shall see, however, this disturbance affects mainly the tail of the distribution function. Hence it can be expected that the above correction factors apply also in the case of kinetic non-equilibrium. Secondly, the gain and the loss terms in the reactive collision integral are weighted with the same factor $k^{(0)}_\mathrm{f}/\tilde{k}^{(0)}_\mathrm{f}$. (In the case of a separate weighting with $k^{(0)}_\mathrm{f}/\tilde{k}^{(0)}_\mathrm{f}$ and $k^{(0)}_r/\tilde{k}^{(0)}_\mathrm{r}$, the conservation laws and the H-theorem would be violated in the numerical scheme.) This falsification of the loss term is of no consequence, if the reverse reaction rate has only minor influence on the history of the process, as is the case for the combustion-type reactions considered in this paper.

The numerical results presented in the next paragraph were obtained with a cut-off energy given by equation (3.26) and a grid point number N such that $\Delta x \approx \kappa T^\mathrm{eq}$. A mesh size of approximately κT^eq was found to be sufficient for a satisfactory convergence of the numerical scheme.

4. Numerical results

(*a*) *Very fast reactions*

For the numerical solution of equation (3.30) the standard techniques for ODEs can be applied. For activation energies E^*_f less than approximately $8\kappa T_0$, the classical Runge–Kutta method and the explicit midpoint-rule with polynomial extrapolation proved to be efficient. Both methods, however, are useless if the system (3.30) is stiff. Stiffness arises if the typical time for chemical relaxation is much slower than the translational relaxation time. This is caused by high activation energies ($E^*_\mathrm{f} \gtrsim 8\kappa T_0$). In that case, equation (3.30) was solved by means of the package LSODE by Hindmarsh which is based on a variable-order backward differentiation formula (cf. Fatunla 1988). The chemical rate equation (2.21) was solved by means of Runge–Kutta for all ranges of parameters.

In presenting numerical results we begin with 'very fast reactions', i.e. reactions which are completed after only some ten collision times. This is the case for low activation energy, $E^*_\mathrm{f} \lesssim 3\kappa T_0$. As a reference time, here and in the following the

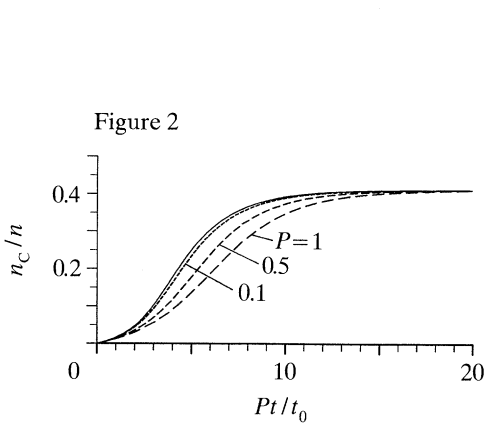

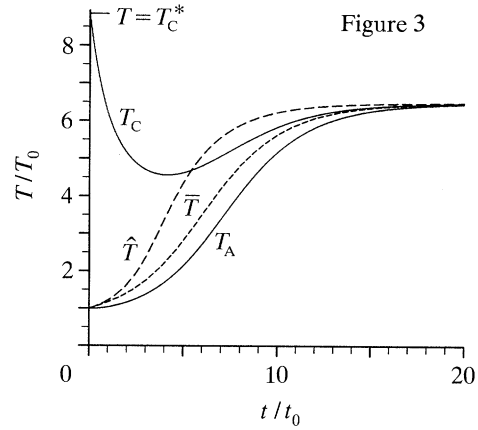

Figure 2. Product density against time. Solid curve, solution of the chemical rate equation using the Arrhenius law; dashed curves, densities obtained from solutions of the Boltzmann equation for various values of the steric factor; $Q = 20\kappa T_0$, $E_f^* = 3\kappa T_0$.

Figure 3. Temperature against time. T_A, T_C and $\bar{T}$, species temperatures and mean temperature obtained from Boltzmann equation; $\hat{T}$, temperature according rate equation. $Q = 20\kappa T_0$, $E_f^* = 3\kappa T_0$ $P = 1$.

initial mean collision time

$$t_0 = \nu(T_0)^{-1} \tag{4.1}$$

is used, with the collision frequency ν given by equation (2.25). Figure 2 shows the time evolution of the reactant density for a very fast reaction with high heat of reaction. A considerable deviation of the kinetic theory based density profile from the one obtained with the chemical rate equation can be seen. For the solution of the rate equation (2.21), the Arrhenius rate constants (2.24) were used, with the temperature taken from equation (2.22). For a steric factor $P = 1$, the reaction proceeds more slowly if predicted by the Boltzmann equation. However, as P is decreased, the results of the two different descriptions converge quickly.

Figure 3 displays the change in temperature during the reaction. In the fast process under consideration, the product molecules find not enough time to transfer all their excess energy to reactant molecules. As a result, the product temperature is much higher than the one of the reactants throughout the reaction. One striking thing is a kind of 'initial boundary layer' in the product temperature T_C. As shown in Appendix B, the mean energy of a C or D particle emerging from a reactive encounter is

$$E_{C,D}^{(+)} = \tfrac{1}{2}(Q + E_f^*) + \tfrac{7}{4}\kappa T, \tag{4.2}$$

where T is the temperature of the reactants. At the very start of the reaction, the components C and D are made up entirely by hot molecules. Hence one finds for the temperature of the product particles in the beginning of the reaction

$$\frac{T_C^*}{T_0} = \frac{2E_{C,D}^{(+)}}{3\kappa T_0} = \frac{Q + E_f^*}{3\kappa T_0} + \frac{7}{6}, \tag{4.3}$$

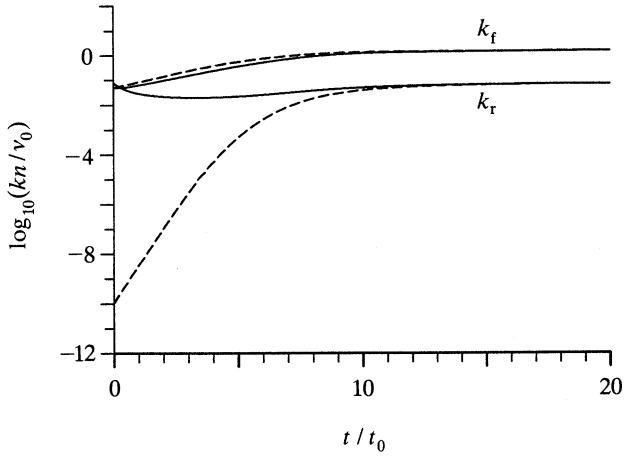

Figure 4. Rate constants against time. Solid curves, rate constants obtained from Boltzmann equation; dashed curves, Arrhenius rate constants; parameters as in figure 3.

which is in agreement with the numerical value obtained from the Boltzmann equation.

Once formed, C and D particles slow down in the 'cold' reactant gas. In the course of time, molecules which have already suffered a few collisions start to dominate the average kinetic energy of the C and D components. In the present case, however, the reaction is too fast for an assimilation of the product and reactant temperatures before chemical equilibrium is reached. Figure 3 also displays the mean temperaure

$$\bar{T} = \frac{1}{n} \sum_{\alpha=\mathrm{A},\ldots,\mathrm{D}} n_\alpha T_\alpha = \frac{n_\mathrm{A} T_\mathrm{A} + n_\mathrm{C} T_\mathrm{C}}{n_\mathrm{A} + n_\mathrm{C}}, \tag{4.4}$$

as well as the temperature according to the rate equation, $\hat{T}$. The latter shows a faster equilibration than the 'Boltzmann' temperature $\bar{T}$, which is in accordance with the density plot.

Next we consider the time evolution of the rate constants (see figure 4). The equilibrium values are taken from the Arrhenius law (2.24) with $T = \bar{T}$. The non-equilibrium rate constants are defined by

$$k_\mathrm{f}(t) = \frac{1}{n_\mathrm{A} n_\mathrm{B}} \frac{k_\mathrm{f}^{(0)}}{\tilde{k}_\mathrm{f}^{(0)}} \sum_{i,k,l=1}^{N} \left(R_\mathrm{AB}^\mathrm{CD}\right)_{kl}^{i} G_\mathrm{A}^k(t) G_\mathrm{B}^l(t), \tag{4.5}$$

$$k_\mathrm{r}(t) = \frac{1}{n_\mathrm{C} n_\mathrm{D}} \frac{k_\mathrm{f}^{(0)}}{\tilde{k}_\mathrm{f}^{(0)}} \sum_{i,k,l=1}^{N} \left(R_\mathrm{CD}^\mathrm{AB}\right)_{kl}^{i} G_\mathrm{C}^k(t) G_\mathrm{D}^l(t), \tag{4.6}$$

with $G_\alpha^i(t)$ being the solution of the multigroup equations. Equation (4.5) is the discretized version of the definition of the forward rate constant (2.23). For a discussion of the numerical correction factor $k_\mathrm{f}^{(0)}/\tilde{k}_\mathrm{f}^{(0)}$ see § 3 *e*. As can be seen from figure 4, the equilibrium forward rate constant $k_\mathrm{f}^{(0)}$ is slightly higher than

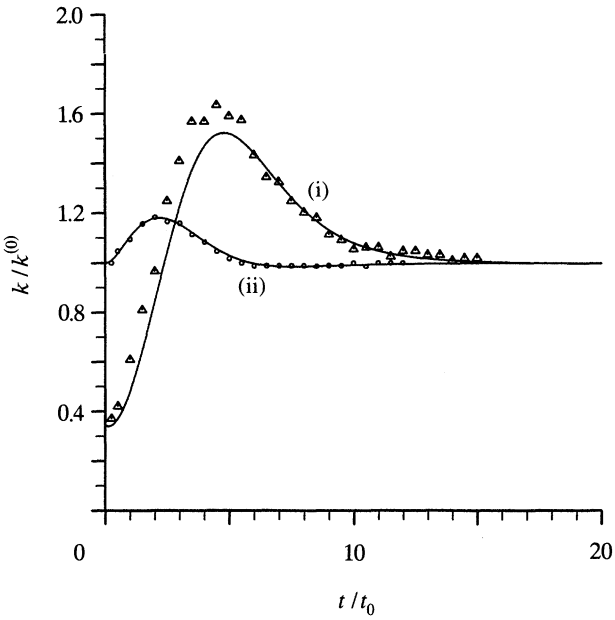

Figure 5. Ratio of actual rate constant and Arrhenius rate constant against time; (i) $k_r/k_r^{(0)}(T_C)$; (ii) $k_f/k_f^{(0)}(T_A)$; symbols, Monte Carlo results by Koura (1973); parameters as in figure 3.

k_f throughout the reaction process, which causes the solution of the chemical rate equation to reach equilibrium faster than the outcome of the Boltzmann equation (see figure 2). The reason for this difference lies in the fact that the mean temperature $\bar{T}$ which enters $k_f^{(0)}$ is higher than the species temperature T_A. As far as the reaction products are concerned, the opposite applies. Here the species temperature T_C is much higher than $\bar{T}$. As a result k_r is larger than $k_r^{(0)}$ by some orders of magnitude (see figure 4). This huge difference, however, has only minor implications on the history of the process. Despite the increased reverse rate constant, the reverse reaction *rate* is only small compared to the forward rate during the interval $0 \leq t \lesssim 8t_0$.

Finally, the ratio of non-equilibrium and equilibrium rate constants is considered, but now with reference to the species temperatures rather than to the mean temperature (see figure 5). Such an illustration of the non-equilibrium rate constants was chosen by Koura (1973) who solved the Boltzmann equation for a very similar model gas by means of a Monte Carlo method. A good agreement of the present results with the Monte Carlo ones can be detected from figure 5.

For a more detailed investigation of very fast reactions, especially for a discussion of the results in terms of non-equilibrium velocity distribution functions, the reader is refered to the work of Koura.

(*b*) *Fast reactions*

We now focus attention on systems with high activation energy ($E_f^* \gtrsim 8\kappa T_0$). In this case, the probability for a reaction between an A and a B particle is small,

$$k_f^{(0)'} = P \exp(-E_f^*/\kappa T_0) \ll 1. \tag{4.7}$$

Chemical equilibration requires therefore many hundreds or thousands of mean collision times. Yet in all cases under consideration in the present paper, the reaction time is small on a macroscopic timescale. Hence we speak of 'fast reactions' with reference to the terminology used in chemical kinetics.

As in the previous subsection, only reactions with large heat of reaction are examined. The solutions of the Boltzmann equation then describe a thermal explosion, as can be seen from figure 6. A thermal explosion is characterized by a relatively long induction period during which the densities and the temperature change only slightly, followed by a sudden increase in product density and temperature. Once the system has 'ignited', it passes into chemical equilibrium, as described by equations (2.8) and (2.9).

An estimate of the ignition time t_i can be obtained from the chemical rate equation in the form of an asymptotic expansion in terms of the small parameter $\kappa T_0/E_f^*$ (see, for example, Strehlow 1988). For the present model gas one finds

$$\frac{t_i}{t_0} = 6\frac{(\kappa T_0)^2}{QE_f^*} \exp\left(\frac{E_f^*}{\kappa T_0}\right)\left(1 + 2\frac{\kappa T_0}{E_f^*} + \dots\right), \tag{4.8}$$

where t_0 is the initial mean collision time defined by equation (4.1). The ignition times depicted by figure 6 are in good agreement with t_i.

However, a comparison of the Boltzmann results with the solution of the chemical rate equation reveals that the kinetic theory model gives a slightly premature ignition. As an example, we consider the parameter case $Q = 20\kappa T_0$, $E_f^* = 10\kappa T_0$ (see figure 7). For decreasing steric factor P, the outcome of the Boltzmann equation converges quickly to that of the rate equation. But for $P = 1$, a shortening of the induction period of about 7% can be seen. This deviation is remarkable if one considers that in the present case initially only one in about 22 000 collisions between A and B particles is reactive.

Before going on with the explanation of this non-equilibrium effect, we briefly discuss the time evolution of the temperatures (figure 8). As in the case of 'very fast reactions', an initial boundary layer in the temperature profile of the reactant molecules can be detected. In the present case, however, where the reaction is slow in terms of the collision frequency, the hot C and D particles have enough time to thermalize in the cold A, B gas. As a result, T_C converges close to T_A in the induction period. Note that when ignition sets in, the product temperature T_C grows faster than the reactant temperature T_A.

For a discussion of the shortening of the ignition time, we next consider the time evolution of the reaction rate constants (figure 9). As in the 'very fast reaction' case, the reverse rate constant obtained from solutions of the Boltzmann equation is hugely increased compared to the Arrhenius law. This non-equilibrium effect, however, has no implications on the reaction process, because the reverse rate can be neglected against the forward rate throughout the induction period. Much more important is the slightly increased forward rate constant. The non-

PHILOSOPHICAL TRANSACTIONS OF THE ROYAL SOCIETY A MATHEMATICAL, PHYSICAL & ENGINEERING SCIENCES

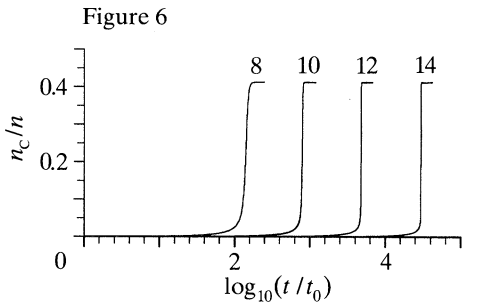

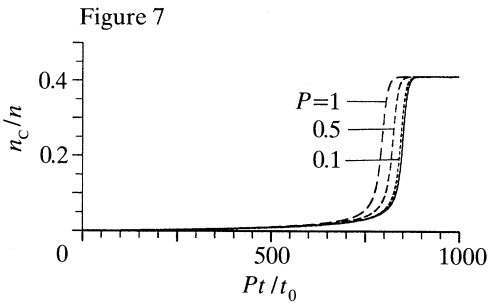

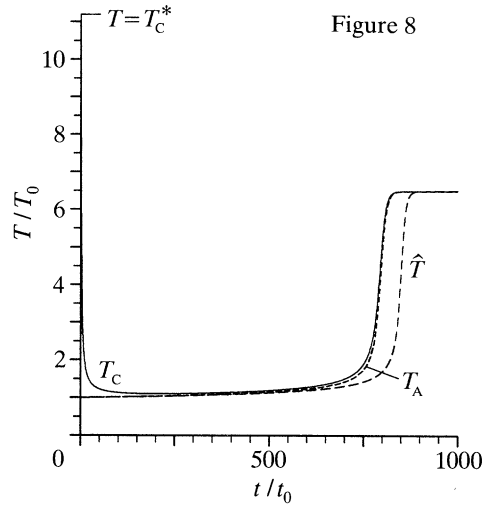

Figure 6. Product density obtained from solutions of the Boltzmann equation against time for various values of E_f^*; $Q = 20\kappa T_0$, $P = 1$.

Figure 7. Product density against time. Solid curve, solution of the chemical rate equation using the Arrhenius law; dashed curves, densities obtained from the Boltzmann equation for various values of the steric factor; $Q = 20\kappa T_0$, $E_f^* = 10\kappa T_0$.

Figure 8. Temperature against time. T_A, T_C, species temperatures obtained from Boltzmann equation; $\hat{T}$, temperature from rate equation. $Q = 20\kappa T_0$, $E_f^* = 10\kappa T_0$, $P = 1$.

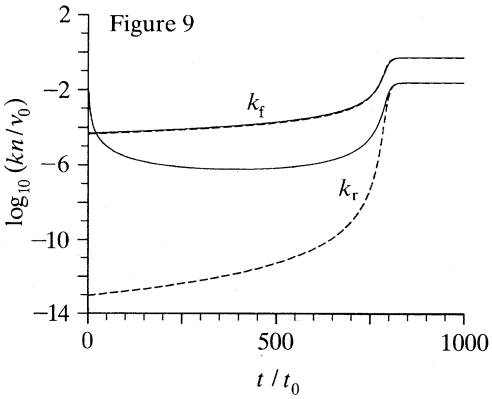

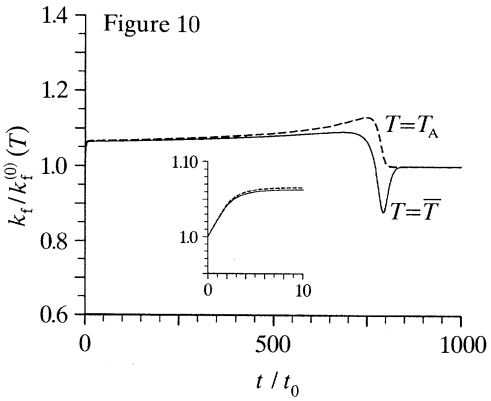

Figure 9. Rate constants against time. Solid curves, rate constants obtained from Boltzmann equation; dashed curves, Arrhenius rate constants; parameters as in figure 8.

Figure 10. Ratio of actual rate constant and Arrhenius rate constant against time; parameters as in figure 8.

PHILOSOPHICAL TRANSACTIONS OF THE ROYAL SOCIETY A MATHEMATICAL, PHYSICAL & ENGINEERING SCIENCES

logarithmic representation given by figure 10 shows that the actual forward rate constant k_f, after an initial stage of relaxation is almost steadily increased compared to the Arrhenius rate $k_f^{(0)}$. This increase, which amounts to approximately 7%, gives rise to the earlier ignition discussed above. Figure 10 displays a kind of oscillation in the profile of $k_f/k_f^{(0)}(\bar{T})$ at the time when the system ignites. This behaviour which has no physical consequences is caused by the slight difference between T_A and T_C (and hence between T_A and $\bar{T}$) during ignition. A plot of $k_f/k_f^{(0)}$ with reference of $k_f^{(0)}$ to T_A rather than to $\bar{T}$ shows no such oscillation (see figure 10).

The reason for the deviation of the rate constants from the Arrhenius law can be found in a kinetic non-equilibrium of the gas particles. Figure 11 shows the velocity distribution function of the product molecules during the initial stage of the reaction. Note that the chosen velocity unit varies with time. In the very beginning of the reaction, f_C has the shape of a gaussian distribution. In order to give an estimate for the molecular velocity $\bar{v}$ for which this 'birth spectrum' of product particles has its maximum, we consider that the mean energy of product particles is initially $E_{C,D}^{(+)}$, given by equation (4.2). For the peaked gaussian shown in figure 11, the square of the mean velocity, $\bar{v}^2$, equals approximately the mean square velocity, $\overline{v^2}$, so that we have

$$\tfrac{1}{2}m\bar{v}^2 \approx \tfrac{1}{2}m\overline{v^2} = E_{C,D}^{(+)}. \tag{4.9}$$

Considering that the initial velocity unit is determined by the temperature T_C^* defined by equation (4.3), we find for the location of the initial peak of the product particle distribution

$$\bar{v}/\sqrt{(2\kappa T_C/m)} = \sqrt{\tfrac{3}{2}}, \tag{4.10}$$

which is in agreement with the location of the maximum of $f_C(t = 0.01t_0)$ (see figure 11). We note that a good fit to the birth spectrum of product particles can be obtained by assuming a gaussian with a mean square velocity given by $\bar{v}^2$ and a mean square fluctuation equal to the one of a maxwellian.

In the course of a few mean collision times, the distribution of product particles tends towards a maxwellian in the thermal velocity range. However, the high energy tail of the distribution function is hugely overpopulated throughout the induction domain, as can be seen from figure 12. This overpopulation causes the huge increase of the reverse reaction rate constant.

We next turn attention to the distribution function of the reactant molecules which is responsible for the increased forward rate constant, and consequently for the earlier ignition. Figure 13 displays the energy distribution $G_A(x,t)$ relative to the equilibrium distribution $G_A^{eq}(x; n_A, T_A)$ at various times during the induction period. A perfect Maxwell distribution in the thermal energy range can be detected, but for particle energies larger than approximately E_f^*, the distribution function is highly overpopulated. Although only small in its absolute amount, this excess of hot particles is sufficient for the noticeable increase of the forward rate constant.

Figure 14*a–d* shows further comparisons of the Boltzmann results with the solution of the chemical rate equation. The Boltzmann equation was not always solved until chemical equilibrium was reached but in some cases only until ignition

PHILOSOPHICAL TRANSACTIONS OF THE ROYAL SOCIETY A MATHEMATICAL, PHYSICAL & ENGINEERING SCIENCES

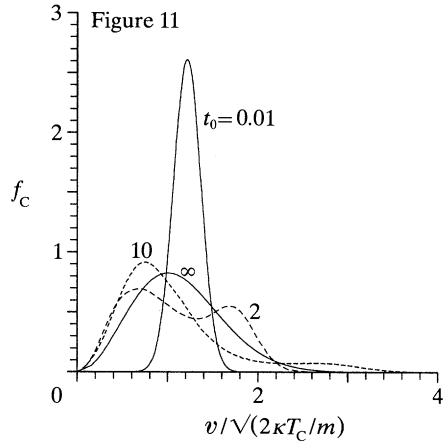

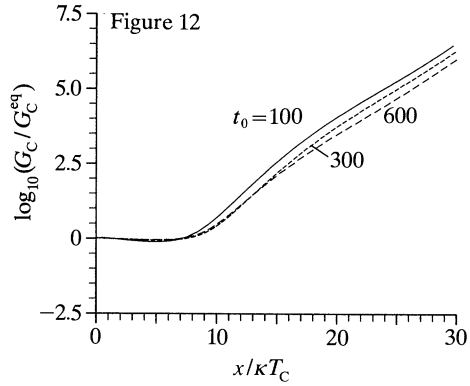

Figure 11. Normalized velocity distribution function of product molecules at various times during the initial boundary layer; parameters as in figure 8.

Figure 12. Energy distribution function of product molecules relative to equilibrium distribution at various times during the induction period; parameters as in figure 8.

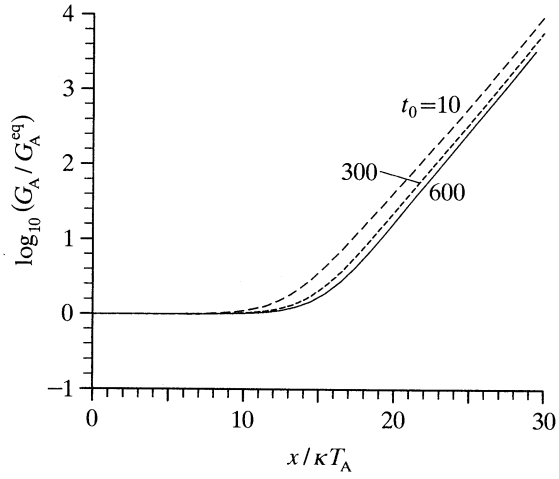

Figure 13. Energy distribution function of reactant molecules relative to equilibrium distribution at various times during the induction period; parameters as in figure 8.

set in. This was done in order to save computing time. If we do not follow the system until the final temperature is reached, a smaller cut-off energy can be used in the numerical method. Therefore a smaller number of grid points can be chosen for a given Δx, which reduces the number of equations in the system (3.30). Such a broken run, however, reveals all the information required for the determination of the non-equilibrium effects in the reacting gas.

It can be seen from the examples presented in figure 14, that the density profiles obtained from the Boltzmann equation and those from the rate equation are

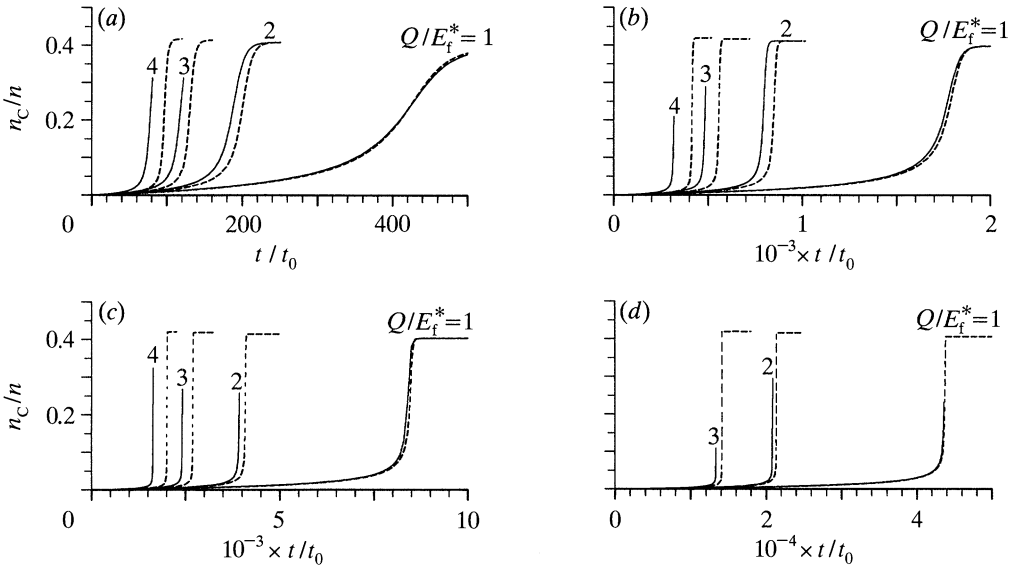

Figure 14. Product density against time. Solid curves, densities obtained from Boltzmann equation; dashed curve, solution of the rate equation using the Arrhenius law; steric factor $P = 1$; (*a*) $E_f^* = 8\kappa T_0$, (*b*) $E_f^* = 10\kappa T_0$, (*c*) $E_f^* = 12\kappa T_0$, (*d*) $E_f^* = 14\kappa T_0$.

approximately the same for $Q = E_f^*$. For $Q \geq 2E_f^*$, however, the induction period is considerably shortened. An earlier ignition can be detected even for $E_f^* = 14\kappa T_0$, where initially only about one in one million collisions between A and B particles is reactive.

We note that the non-equilibrium distribution functions of the reactant particles are in all cases under consideration qualitatively the same as those shown in figure 13. Above E_f^*, the distribution functions are highly overpopulated compared to the equilibrium distribution. In a logarithmic representation this overpopulation increases almost linearly with the particle energy. This suggests that the non-equilibrium distribution function of the reactant particles during the induction period is an overlap of two maxwellians.

5. Summary and discussion of results

The present research shows that in chemical reactions with large heat release the velocity distribution functions may be perturbed to such an extent that the non-equilibrium contributions to the chemical rate constants are noticeable. Both reactions with low activation energy ($E_f^* = 3\kappa T_0$) and with high activation energy ($E_f^* \geq 8\kappa T_0$) have been investigated. In the former case where the reactant and product temperatures are considerably different throughout the reaction process, the reaction proceeds more slowly if predicted by the Boltzmann equation. For high activation energies, on the contrary, the reaction completes faster according to the Boltzmann equation. The reason for this lies in an increase of the forward rate constant caused by an overpopulation of the tail of the reactant particle velocity distribution. In the case of high activation energy and high heat

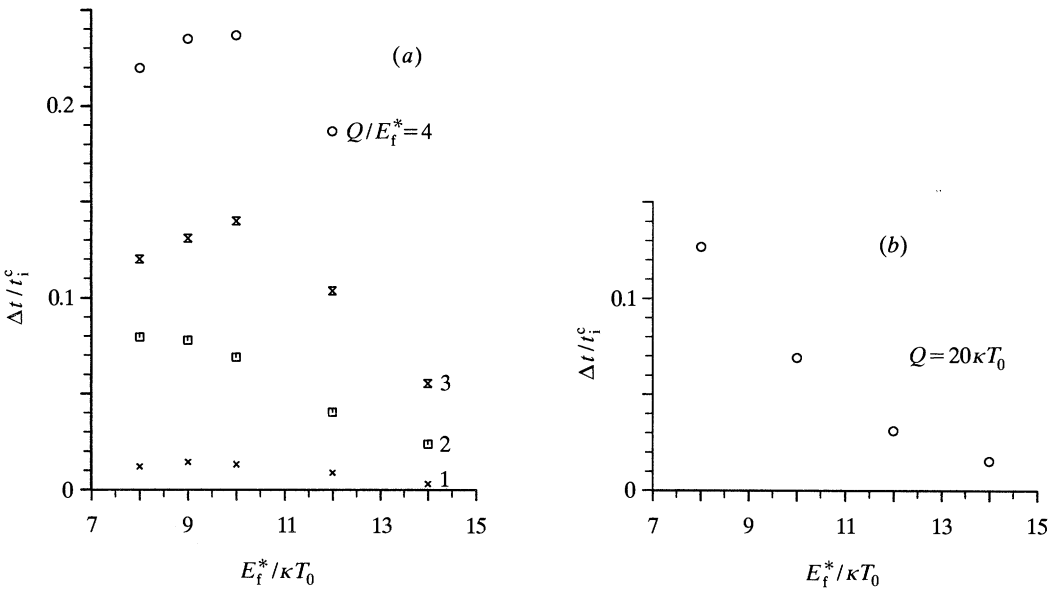

Figure 15. Shortening of the induction period of an adiabatic thermal explosion due to translational non-equilibrium effects; steric factor $P = 1$. $\Delta t = t_i^C - t_i^B$; t_i^B and t_i^C are the ignition times obtained from the Boltzmann equation and the chemical rate equation, respectively.

of reaction, the present model gas undergoes an adiabatic thermal explosion. The increased speed of reaction is equivalent to a shortening of the induction period. Figure 15 displays the relative reduction of the ignition time due to translational non-equilibrium effects in the reacting gas. Ignition is defined as the moment where the product density has reached a fifth of its equilibrium value. For the parameters under consideration here, the shortening of the ignition time can amount to 24%. We conclude therefore that a high activation energy is not sufficient for the equilibrium assumption usually made in the collision theory of chemical reactions, if large heats of reaction ($Q \geq E_f^*$) are taken into account.

So far, however, only the results obtained for a steric factor $P = 1$ have been summarized, whereas in real chemical reactions the steric factors are small. It appears from a number of numerical examples that a decrease of P reduces the extent of the non-equilibrium effects by exactly the same amount (see figures 2 and 7). Hence a small steric factor leads to kinetic equilibrium in the present model situation, even if the disturbances due to reactive encounters are violent.

The numerical calculations were restricted to pure stoichiometric mixtures of reactants and products, in which case the non-equilibrium contributions to the rate constants are the largest. It can be expected that the addition of an inert gas has a similar effect as a reduction of the steric factor, in that the presence of inert molecules reduces the reaction probability per collision of a reactant particle. The same applies if the mixture is not stoichiometric.

In discussing the implications of the present work on chemical kinetics one has to reconsider the assumptions made in the formulation of the model problem. One major assumption was the limitation to a single reaction step. It was found

that the reverse rate constant in this single step is hugely increased as a result of translational non-equilibrium of the product particles. Yet in the present case this increase is of no consequence, since the reverse rate is negligible during the induction period. If the products of a highly exothermic reaction step (1), however, enter a consecutive step (2) with an energy threshhold, such as

$$\begin{array}{ll}(1) & \mathrm{A}+\mathrm{B}\rightarrow\mathrm{C}+\mathrm{D},\\ (2) & \mathrm{C}+\mathrm{D}\rightarrow\mathrm{E}+\mathrm{F},\end{array}$$

this huge increase in the reaction rate of product particles concerns a forward step. In this case the translational non-equilibrium effects may have a crucial influence on the kinetics of the reaction process, even if the steric factors are small.

A second point concerns the restriction to particles without internal degrees of freedom. As became clear in the present research, the small ratio of translational and chemical relaxation times does not necessarily imply that the translational mode can be regarded as being in equilibrium during the reaction process. The vibrational relaxation is much slower than the translational one. Hence a strong overpopulation of high energy vibrational levels can be expected during fast and highly exothermic reactions. The resulting corrections to the Arrhenius rate constants may be much larger than those due to translational non-equilibrium. Further research on the basis of more realistic model systems is encouraged.

I thank Professor J.F. Clarke of the Cranfield Institute of Technology for all his help and advice given during the preparation of this work. The grant of an Erwin Schrödinger fellowship from the Austrian Fonds zur Förderung der wissenschaftlichen Forschung is gratefully acknowledged. My thanks must also go to the British Science and Engineering Research Council for the use of a SUN-Sparc station on which the numerical calculations were performed.

Appendix A. Evaluation of scalar scattering kernels

As stated in § 3 *a*, the multiple integral (3.5) can be reduced to a onefold integral (cf. Kügerl 1991). After lengthy but elementary manipulations one obtains instead of equation (3.5)

$$R^{\alpha\beta}_{\gamma\delta}(x'_1,x'_2|x_1)=\tfrac{1}{2}m^{5/2}\int_{z_1}^{z_2}\mathrm{d}E\,\frac{E^{1/2}\,\sigma^{\alpha\beta}_{\gamma\delta}(E)}{(E+Q^{\alpha\beta}_{\gamma\delta})^{1/2}(x'_1+x'_2-E)^{1/2}},\tag{A 1}$$

with the integration limits

$$z_1=\tfrac{1}{2}\max\left[\left(\sqrt{x'_1}-\sqrt{x'_2}\right)^2,(\sqrt{x_1}-\sqrt{x_z})^2-2Q^{\alpha\beta}_{\gamma\delta}\right],\tag{A 2}$$

$$z_2=\tfrac{1}{2}\min\left[\left(\sqrt{x'_1}+\sqrt{x'_2}\right)^2,(\sqrt{x_1}+\sqrt{x_z})^2-2Q^{\alpha\beta}_{\gamma\delta}\right].\tag{A 3}$$

Here and in the following, x_2 is defined by

$$x_2=x'_1+x'_2-x_1+Q^{\alpha\beta}_{\gamma\delta}.\tag{A 4}$$

It is the subject of this appendix to present the results of the evaluation of integral (A 1) for the various cross sections introduced in § 2 *b*.

PHILOSOPHICAL TRANSACTIONS OF THE ROYAL SOCIETY A MATHEMATICAL, PHYSICAL & ENGINEERING SCIENCES

(*a*) *Hard spheres*

For a series of elastic transitions, such as (A,A)→(A,A), the cross section is assumed to be constant (see equation (2.18)). Considering that in the case of elastic scattering $Q_{\gamma\delta}^{\alpha\beta} = 0$, the evaluation of equation (A 1) is elementary. The result can be presented in the form

$$R_{\mathrm{AA}}^{\mathrm{AA}}(x_1', x_2'|x_1) = (2m^5)^{1/2}\sigma \min(x_1', x_2', x_1, x_1' + x_2' - x_1)^{1/2}\, \Theta(x_1' + x_2' - x_1), \tag{A 5}$$

where Θ denotes Heaviside's step function.

(*b*) *Reactive hard spheres*

For the reactive process (A,B)→(C,D), with $Q_{\mathrm{AB}}^{\mathrm{CD}} = Q$, the line-of-centres cross section (2.14) applies. Also in this case a closed analytic evaluation of equation (A 1) is possible by using the elliptic integrals of first and second kind (Abramowitz & Stegun 1970),

$$F(\lambda, p) = \int_0^{\sin\lambda} \mathrm{d}x\, (1 - x^2)^{-1/2}(1 - px^2)^{-1/2}, \tag{A 6}$$

and

$$E(\lambda, p) = \int_0^{\sin\lambda} \mathrm{d}x\, (1 - x^2)^{-1/2}(1 - px^2)^{1/2}, \tag{A 7}$$

respectively. The result is

$$\begin{aligned} R_{\mathrm{AB}}^{\mathrm{CD}}(x_1', x_2'|x_2) = {} & P\sigma m^{5/2}\Theta_1\Theta_2\Theta_3 \\ & \times\Big\{(x_1' + x_2' + Q)^{1/2}\,[E(\lambda_1, p) - E(\lambda_2, p)] \\ & - \frac{Q + E_f^*}{(x_1' + x_2' + Q)^{1/2}}\,[F(\lambda_1, p) - F(\lambda_2, p)]\Big\}. \end{aligned} \tag{A 8}$$

Here, the abbreviations

$$p = \frac{x_1' + x_2'}{x_1' + x_2' + Q}, \qquad \lambda_{1,2} = \arcsin\left(\frac{x_1' + x_2' - s_{1,2}}{x_1' + x_2'}\right)^{1/2}, \tag{A 9}$$

$$s_1 = \tfrac{1}{2}\max\left[\left(\sqrt{x_1'} - \sqrt{x_2'}\right)^2, (\sqrt{x_1} - \sqrt{x_z})^2 - 2Q, 2E_f^*\right], \tag{A 10}$$

$$s_2 = \tfrac{1}{2}\min\left[\left(\sqrt{x_1'} + \sqrt{x_2'}\right)^2, (\sqrt{x_1} + \sqrt{x_z})^2 - 2Q\right] \tag{A 11}$$

have been used. The three Θ-functions in equation (A 8) are defined by:

$$\Theta_1 = \Theta(x_1' + x_2' - x_1 + Q), \tag{A 12}$$

$$\Theta_2 = \Theta[(x_1'x_2')^{1/2} + (x_1x_2)^{1/2} - \tfrac{1}{2}Q], \tag{A 13}$$

$$\Theta_3 = \Theta(s_2 - E_f^*). \tag{A 14}$$

The evaluation of equation (A 1) for the transition (C,D)→(A,B), with $Q_{\mathrm{CD}}^{\mathrm{AB}} = -Q$, leads to a similar result. However, because of the principle of microscopic

reversibility (cf. Kügerl 1991), the scalar scattering kernel R_{CD}^{AB} can readily be obtained in terms of R_{AB}^{CD}:

$$R_{CD}^{AB}(x_1', x_2'|x_2) = R_{AB}^{CD}(x_1, x_1' + x_2' - x_1 - Q|x_1'). \tag{A 15}$$

(*c*) *Elastic scattering with non-constant cross section*

Evaluation of equation (A 1) for the elastic transition (A,B)→(A,B) with the cross section given by equation (2.19) yields

$$\begin{aligned} R_{AB}^{AB}(x_1', x_2'|x_1) = R_{AA}^{AA}(x_1', x_2'|x_1) - \tfrac{1}{2} P\sigma m^{5/2} \Theta_1 \Theta_3 \\ \times \Bigg\{ 2\left[(x_1' + x_2' - s_1)^{1/2} - (x_1' + x_2' - s_2)^{1/2}\right] \\ - \frac{E_f^*}{(x_1' + x_2')^{1/2}} \left[\ln \frac{(x_1' + x_2')^{1/2} + (x_1' + x_2' - s_1)^{1/2}}{(x_1' + x_2')^{1/2} - (x_1' + x_2' - s_1)^{1/2}} \right. \\ \left. - \ln \frac{(x_1' + x_2')^{1/2} + (x_1' + x_2' - s_2)^{1/2}}{(x_1' + x_2')^{1/2} - (x_1' + x_2' - s_2)^{1/2}} \right] \Bigg\}. \end{aligned} \tag{A 16}$$

The abbreviations s_1, s_2, Θ_1 and Θ_3 are defined by equations (A 10), (A 11), (A 12) and (A 14), respectively, with $Q = 0$. The result for R_{CD}^{CD} is the same as (A 16), except that E_r^* has to be used in equations (A 10), (A 14) and (A 16), instead of E_f^*.

Appendix B. Mean energy of reaction products

We finally state a few mean energies involved in the binary reaction process. To calculate the mean energy of the product particles emerging from a reactive collision, we start with the energy which is lost on average if an A and a B particle react:

$$E^{(-)} = \frac{\int \mathrm{d}\boldsymbol{v}_1 \int \mathrm{d}\boldsymbol{v}_2 \left(\frac{1}{2} m {v_1}^2 + \frac{1}{2} m {v_2}^2\right) g \sigma_f f_A(\boldsymbol{v}_1) f_B(\boldsymbol{v}_2)}{\int \mathrm{d}\boldsymbol{v}_1 \int \mathrm{d}\boldsymbol{v}_2 \, g \sigma_f f_A(\boldsymbol{v}_1) f_B(\boldsymbol{v}_2)}, \tag{B 1}$$

with $g = |\boldsymbol{v}_1 - \boldsymbol{v}_2|$. Assuming an equilibrium distribution for f_A and f_B and using the reactive hard sphere model (2.14), the integral equation (B 1) can be evaluated after a transformation to centre-of-mass coordinates. One finds for the mean energy of an A or B particle entering a reactive collision:

$$E_{A,B}^{(-)} = \tfrac{1}{2} E^{(-)} = \tfrac{1}{2} E_f^* + \tfrac{7}{4} \kappa T. \tag{B 2}$$

The mean energy of a C or D particle emerging from a reactive collision, $E_{C,D}^{(+)}$, can now be obtained by considering that the total postcollisional kinetic energy is the sum of the precollisional energy and the heat of reaction. The result is given by equation (4.2).

References

Abramowitz, M. & Stegun, I. A. 1970 *Handbook of mathematical functions.* New York: Dover.

Bell, G. I. & Glasstone, S. 1970 *Nuclear reactor theory.* New York: Van Nostrand Reinhold.

Boffi, V. C. & Rossani, A. 1990 On the Boltzmann system for a mixture of reacting gases. *J. appl. math. Phys. (ZAMP)* **41**, 254–269.

Ernst, M. H. 1981 Nonlinear model-Boltzmann equations and exact solutions. *Phys. Rep.* **78**, 1–171.

Fatunla, S. O. 1988 *Numerical methods for initial value problems in ordinary differential equations.* Boston: Academic Press.

Kondrat'ev, V. N. 1964 *Chemical kinetics of gas reactions.* Oxford: Pergamon Press.

Koura, K. 1973 Nonequilibrium velocity distributions and reaction rates in fast highly exothermic reactions. *J. chem. Phys.* **59**, 691–697.

Kügerl, G. 1989 Laguerre polynomial solution of the nonlinear Boltzmann equation for the hard-sphere model. *J. appl. math. Phys. (ZAMP)* **40**, 816–827.

Kügerl, G. & Schürrer, F. 1990 Multigroup solutions of the nonlinear Boltzmann equation. *Phys. Fluids* A**2**, 2204–2210.

Kügerl, G. 1991 A consistent numerical method for the solution of the nonlinear Boltzmann equation for inelastic and reactive scattering. *J. appl. math. Phys. (ZAMP)* **42**, 821–836.

Light, J. C., Ross, J. & Shuler, K. E. 1969 Rate coefficients, reaction cross sections and microscopic reversibility. In *Kinetic processes in gases and plasmas* (ed. A. R. Hochstim), pp. 281–320. New York and London: Academic Press.

Polak, L. S. & Khachoyan, A. V. 1985 Generalization of Boltzmann's H-theorem for a reacting gas mixture. *Soviet J. chem. Phys.* **2**, 1474–1485.

Prigogine, I. & Mahieu, M. 1950 Sur la perturbation de la distribution de Maxwell par des réactions chimiques en phase gazeuse. *Physica* **16**, 51–64.

Pyun, C. W. & Ross, J. 1964 Composition dependence of nonequilibrium effects in gas-phase reactions. *J. chem. Phys.* **40**, 2572–2583.

Ross, J. & Mazur, P. 1961 Some deductions from a formal statistical mechanical theory of chemical kinetics. *J. chem. Phys.* **35**, 19–28.

Shizgal, B. & Karplus, M. 1970 Nonequilibrium contributions to the rate of reaction. I. Perturbation of the velocity distribution function. *J. chem. Phys.* **52**, 4262–4278.

Shizgal, B. 1971 Nonequilibrium contributions to the rate of reaction. IV. Explicit time-dependent solutions. *J. chem. Phys.* **55**, 76–83.

Strehlow, R. A. 1985 *Combustion fundamentals.* New York: McGraw-Hill.

Ziff, R. M. 1980 New class of soluble-model Boltzmann equations. *Phys. Rev. Lett.* **45**, 306–310.

Received 27 September 1991; revised 6 January 1992; accepted 3 June 1992

PHILOSOPHICAL TRANSACTIONS OF THE ROYAL SOCIETY A MATHEMATICAL, PHYSICAL & ENGINEERING SCIENCES